

Coverage and Rate Analysis for Unmanned Aerial Vehicle Base Stations with LoS/NLoS Propagation

Mohamed Alzenad and Halim Yanikomeroglu

Department of Systems and Computer Engineering, Carleton University, Ottawa, ON, Canada

Email: {mohamed.alzenad, halim}@sce.carleton.ca

Abstract—The use of unmanned aerial vehicle base stations (UAV-BSs) as airborne base stations has recently gained great attention. In this paper, we model a network of UAV-BSs as a Poisson point process (PPP) operating at a certain altitude above the ground users. We adopt an air-to-ground (A2G) channel model that incorporates line-of-sight (LoS) and non-line-of-sight (NLoS) propagation. Thus, UAV-BSs can be decomposed into two independent inhomogeneous PPPs. Under the assumption that NLoS and LoS channels experience Rayleigh and Nakagami- m fading, respectively, we derive approximations for the coverage probability and average achievable rate, and show that these approximations match the simulations with negligible errors. Numerical simulations have shown that the coverage probability and average achievable rate decrease as the height of the UAV-BS increases.

Index Terms—unmanned aerial vehicles, drone, coverage, stochastic geometry.

I. INTRODUCTION

Flexible and easy-to-deploy solutions to provide wireless connectivity are of vital importance in current and future wireless systems. Therefore, the use of unmanned aerial vehicle base stations (UAV-BSs) to enhance coverage or boost capacity has recently attracted great attention [1], [2]. UAV-BSs can assist the terrestrial wireless network in a variety of scenarios. For example, UAV-BSs can be quickly deployed during the aftermath of a natural disaster or to offload traffic from a congested terrestrial BS during a sports event [3]–[5]. Recently, there have been several works on UAV-BS deployment, e.g., [6]–[9]. The authors in [6] proposed a framework for evaluating the 3D location of the UAV-BS that maximizes the number of covered users using minimum transmit power while the work in [7] investigated the 3D placement problem for different QoS requirements. In [8], the authors developed a grid search algorithm to address a backhaul-aware 3D UAV-BS placement problem. A framework for 3D UAV-BSs deployment based on circle packing was proposed in [9]. Moreover, the authors in [9] derived the coverage probability as a function of altitude and antenna gain. However, the work in [6]–[9] aimed at finding the exact 3D location which may be unnecessary and difficult to obtain.

Stochastic geometry has been widely used to model and analyze terrestrial wireless networks. However, a handful of works adopted such approach for UAV-assisted networks. An exact analytical expression for the coverage probability of uniformly distributed UAV-BSs was derived in [10]. This work adopted a terrestrial channel model for the A2G channels and

assumed that all wireless links are subject to Nakagami- m fading. The work in [11] modeled the UAV-BSs as a 2D Binomial point process (BPP) in a disc located at a fixed altitude. The authors assumed that all the UAV-BSs are in LoS condition with the users and hence Nakagami- m fading was assumed for all wireless links. Additionally, the thermal noise was assumed negligible in comparison to interference (interference-limited scenario). The exact coverage probability, and accurate coverage probability approximation for Nakagami- m and fading-free channels were also derived. The authors in [12] investigated spectrum sharing between UAV-BSs and a terrestrial cellular network using tools from stochastic geometry. The UAV-BSs were modeled as a 3D PPP with a minimum height while the terrestrial cellular network was assumed to form a 2D PPP. Additionally in [12], it was assumed that all the UAV-BSs undergo Rayleigh fading which is justified for NLoS transmissions. A network comprised of a single terrestrial BS and a single UAV-BS was investigated in [13]. The authors derived analytical expressions for the uplink coverage probability of a terrestrial BS and a UAV-BS.

Contributions: We adopt an A2G channel model that captures both LoS and NLoS transmissions. Although Rayleigh fading assumption is common for NLoS channels, it may not be for LoS channels. Therefore, we adopt the Nakagami- m distribution for LoS channels. We derive the distribution of the distances from the typical user to the closest NLoS and LoS UAV-BSs. After that, we derive a closed-form expression for the Laplace transform of the aggregated interference power as a function of the altitude and density of UAV-BSs. Unlike the works [10], [11] in which the evaluation of the coverage probability involves finding m numerical derivatives of the Laplace transform of the interference, we derive tractable approximations for the coverage probability and average achievable data rate using bounds on incomplete Gamma function. We show that the approximate coverage probability and average achievable data rate match the simulations very closely.

II. SYSTEM MODEL

We consider a network of UAV-BSs and focus on the analysis of the downlink performance. The UAV-BSs are assumed to be uniformly distributed on an infinite plane located at some altitude h [m] as depicted in Fig. 1. We assume that the UAV-BSs form a homogeneous PPP, denoted by $\Phi \triangleq \{x_i\}$, with density λ [BS/km²] where x_i refers to the 3D location

TABLE I: Notation and Symbols Summary

Notation	Description
PPP	Poisson point process
A2G	Air-to-Ground
h	Height of UAV-BSs
$\Phi; \lambda$	PPP of UAV-BSs; density of UAV-BSs
$x_i; x_o$	3D location of UAV-BS i ; 3D location of serving UAV-BS
$\Phi^N; \Phi^L$	PPP of NLoS UAV-BSs; PPP of LoS UAV-BSs
$P_N(z); P_L(z)$	Probability of NLoS; probability of LoS
m	Parameter of Nakagami- m distribution for LoS links
$D_{N,x_i}; D_{L,x_i}$	Distance between the typical user and a NLoS UAV-BS, or a LoS UAV-BS located at point x_i , respectively
H_{x_i}	Channel power gain between the typical user and a NLoS UAV-BS located at point x_i
G_{x_i}	Channel power gain between the typical user and a LoS UAV-BS located at point x_i
α_N, α_L	Path loss exponent for NLoS, and LoS links, respectively
$P_t; \sigma^2$	Transmit power of UAV-BSs; thermal noise power
η_N, η_L	Additional losses for NLoS, and LoS links, respectively
R_N, R_L	Distance between the typical user and the closest NLoS, and LoS UAV-BS, respectively
$f_{R_N}(r), f_{R_L}(r)$	Distribution of the distance between the typical user and the closest NLoS, and LoS UAV-BS, respectively
$I; \mathcal{L}_I(s r)$	Interference; Laplace transform of interference at s
A_N, A_L	Probability that the typical user is associated with a NLoS UAV-BS, or a LoS UAV-BS, respectively
$P_C; \tau$	Probability of coverage; average downlink rate
$P_{C,N}, P_{C,L}$	Coverage probability given that the typical user is associated with a NLoS, or a LoS UAV-BS, respectively
T	SINR threshold for successful communication
τ_N, τ_L	Average rate given that the typical user is associated with a NLoS, or a LoS UAV-BS, respectively

of the UAV-BS i . Also, we assume that all the UAV-BSs transmit at the same power P_t and a frequency reuse of 1 is used. This implies that the UAV-BSs interfere with each other. However, within a cell, we assume that orthogonal transmission is implemented which implies that intra-cell interference does not occur. Thus, the typical user does not receive interference signals from its serving BS. Without loss of generality, we consider a typical user located at the origin O .

A. Channel Model

The links between the UAV-BSs and the ground users are mainly LoS or NLoS [14]. For a given altitude h , the occurrence of LoS and NLoS transmissions can be captured using the probability of LoS transmission, denoted by $P_L(z)$, and the probability of NLoS transmission, denoted by $P_N(z)$, where [14]

$$P_L(z) = \frac{1}{1 + a \exp(-b(\frac{180}{\pi} \tan^{-1}(\frac{h}{z}) - a))}, \quad (1)$$

where a and b are constants that depend on the environment, and z denotes the Euclidean horizontal distance between the typical user and the projection of the UAV-BS location on the horizontal plane. Furthermore, the probability of NLoS is $P_N(z) = 1 - P_L(z)$.

In our model, we assume that each UAV-BS is either in a LoS or NLoS condition with the typical user and that LoS and NLoS transmissions are independent from each other. This

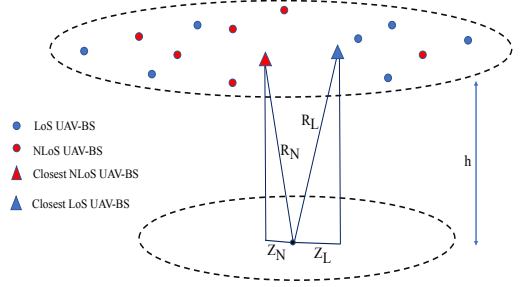


Fig. 1: Illustration of the system model.

implies that the set of UAV-BSs Φ can be decomposed into two independent inhomogeneous PPPs, i.e., $\Phi = \Phi^L \cup \Phi^N$, where Φ^L and Φ^N denote the set of LoS and NLoS UAV-BSs, respectively. Note that the resultant PPPs (Φ^L and Φ^N) are inhomogeneous because $P_L(z)$ and $P_N(z)$ are functions of z . Clearly, for a given altitude h , a UAV-BS with a large horizontal distance z is more likely to be in a NLoS condition with the typical user.

We assume that NLoS and LoS transmissions are characterized by different small scale fading. In particular, we assume that the fading loss, denoted by H_{x_i} , between a NLoS UAV-BS located at point x_i and the typical user is exponentially distributed (Rayleigh fading), i.e., $H_{x_i} \sim \exp(1), \forall x_i \in \Phi^N$. For LoS transmissions, we choose the well known Nakagami- m distribution with the shape parameter m which can capture a wide range of fading scenarios. As a result, the channel fading power gain for LoS links, denoted by G_{x_i} , follows Gamma distribution with probability density function given by [15]

$$f_{G_{x_i}}(g) = \frac{m^m g^{m-1}}{\Gamma(m)} e^{-mg}, \quad \forall x_i \in \Phi^L, \quad (2)$$

where $\Gamma(m)$ is the Gamma function given by $\Gamma(m) = \int_0^\infty x^{m-1} e^{-x} dx$.

Let η_N and η_L denote the mean additional losses for NLoS and LoS transmissions, respectively [14]. The received power at the typical user from a UAV-BS located at point x_i is given by

$$P_{x_i} = \begin{cases} \zeta_N H_{x_i} D_{N,x_i}^{-\alpha_N}, & \forall x_i \in \Phi^N \\ \zeta_L G_{x_i} D_{L,x_i}^{-\alpha_L}, & \forall x_i \in \Phi^L, \end{cases}$$

where $\zeta_N = P_t \eta_N$, and $\zeta_L = P_t \eta_L$. Also, D_{N,x_i} and D_{L,x_i} are the distances between a UAV-BS located at point x_i and the typical user for NLoS and LoS transmissions, respectively. Finally, α_N and α_L are the path loss exponents for NLoS and LoS transmissions, respectively. The notation and symbols used in this paper are summarized in Table I.

B. SINR and UAV-BS Association

The signal-to-interference-plus-noise ratio (SINR) at the typical user when it is associated with a UAV-BS located at

$x_o \in \{\Phi^{\text{LoS}}, \Phi^{\text{NLoS}}\}$ is given by

$$\text{SINR} = \begin{cases} \frac{\zeta_N H_{x_o} R_N^{-\alpha_N}}{\sigma^2 + I}, & \text{if } x_o \in \Phi^N \\ \frac{\zeta_L G_{x_o} R_L^{-\alpha_L}}{\sigma^2 + I}, & \text{if } x_o \in \Phi^L, \end{cases} \quad (3)$$

where R_N and R_L are the distances between the serving UAV-BS and the typical user for NLoS and LoS transmissions, respectively, and σ^2 is the additive white Gaussian noise (AWGN) power. Finally, I is the aggregate interference power defined as

$$I = \sum_{x_i \in \Phi^N/x_o} \zeta_N H_{x_i} D_{N,x_i}^{-\alpha_N} + \sum_{x_i \in \Phi^L/x_o} \zeta_L G_{x_i} D_{L,x_i}^{-\alpha_L}. \quad (4)$$

For the association criteria, we assume that the typical user is associated with the UAV-BS that provides the strongest average SINR. The closest UAV-BS does not necessarily provide the strongest SINR due to the differences in path loss parameters between LoS and NLoS transmissions. In particular, a LoS UAV-BS may provide a stronger average SINR than that provided by a closer NLoS UAV-BS due to the fact that $\eta_L > \eta_N$ and $\alpha_L < \alpha_N$. Moreover, an interfering UAV-BS may provide a higher instantaneous SINR for the typical user than that provided by the serving UAV-BS because of a higher small scale fading in comparison to that experienced by the serving UAV-BS.

Based on the strongest average SINR association scheme and the assumption that $\mathbb{E}[H_{x_i}] = \mathbb{E}[G_{x_i}] = 1, \forall x_i \in \Phi$, the serving UAV-BS can be written as

$$x_o = \arg \max \{ \eta_N R_N^{-\alpha_N}, \eta_L R_L^{-\alpha_L} \}, \quad (5)$$

where $R_N = \min_{x_i \in \Phi^N} D_{N,x_i}$, and $R_L = \min_{x_i \in \Phi^L} D_{L,x_i}$.

III. RELEVANT DISTANCE DISTRIBUTIONS AND ASSOCIATION PROBABILITIES

In this section, we provide the distribution of the distances between the typical user and the closest UAV-BS for NLoS and LoS transmissions. Furthermore, we characterize the location of the closest interfering NLoS and LoS UAV-BSs given that the typical user is associated with a NLoS or a LoS UAV-BS. Finally, we derive expressions for the association probabilities.

Lemma 1. *The probability density function of the distances between the typical user and the closest NLoS and LoS UAV-BSs, denoted by $f_{R_N}(r)$ and $f_{R_L}(r)$, respectively, are given by*

$$f_{R_N}(r) = 2\pi\lambda r P_N(r) \exp\left(-2\pi\lambda \int_0^{l(r)} z P_N(z) dz\right) \quad (6)$$

$$f_{R_L}(r) = 2\pi\lambda r P_L(r) \exp\left(-2\pi\lambda \int_0^{l(r)} z P_L(z) dz\right), \quad (7)$$

where $r \geq h$, $l(r) = \sqrt{r^2 - h^2}$, $P_N(r) = 1 - P_L(r)$, and $P_L(r) = P_L(z)|_{z=\sqrt{r^2-h^2}}$.

Proof. See Appendix A. \square

Corollary 1. *Let Z_N and Z_L denote the horizontal distances between the typical user and the projections of the closest NLoS*

and LoS UAV-BSs on the horizontal plane, respectively. The probability density function of Z_N and Z_L , denoted by $f_{Z_N}(z)$ and $f_{Z_L}(z)$, respectively, are given by

$$f_{Z_N}(z) = 2\pi\lambda z P_N(z) \exp\left(-2\pi\lambda \int_0^z t P_N(t) dt\right) \quad (8)$$

$$f_{Z_L}(z) = 2\pi\lambda z P_L(z) \exp\left(-2\pi\lambda \int_0^z t P_L(t) dt\right). \quad (9)$$

Proof. For Z_N , we have

$$\begin{aligned} F_{Z_N}(z) &= \mathbb{P}(Z_N \leq z) \stackrel{(a)}{=} F_{R_N}(\sqrt{z^2 + h^2}) \\ &\stackrel{(b)}{=} 1 - \exp\left(-2\pi\lambda \int_0^z t P_N(t) dt\right), \end{aligned} \quad (10)$$

where (a) is due to $Z_N = \sqrt{R_N^2 - h^2}$, and (b) follows from (22). Finally, we complete the proof by taking the derivative of $F_{Z_N}(z)$ with respect to z . Following the same steps, we arrive at the final result for $f_{Z_L}(z)$.

The following remarks give clear insight on the range over which the interfering UAV-BSs are located which will be useful when we present the main results of this paper.

Remark 1. *Given that the typical user is associated with a NLoS UAV-BS located at a distance r from the typical user, the closest interfering LoS UAV-BS is at least at a distance*

$$d_L = \left(\frac{\eta_L}{\eta_N}\right)^{\frac{1}{\alpha_L}} r^{\frac{\alpha_N}{\alpha_L}}. \quad (11)$$

Remark 2. *Given that the typical user is associated with a LoS UAV-BS located at a distance r from the typical user, the closest interfering NLoS UAV-BS is at least at a distance*

$$d_N = \begin{cases} h, & \text{if } h \leq r \leq \left(\frac{\eta_L}{\eta_N}\right)^{\frac{1}{\alpha_L}} h^{\frac{\alpha_N}{\alpha_L}} \\ \left(\frac{\eta_N}{\eta_L}\right)^{\frac{1}{\alpha_N}} r^{\frac{\alpha_L}{\alpha_N}}, & \text{if } r > \left(\frac{\eta_L}{\eta_N}\right)^{\frac{1}{\alpha_L}} h^{\frac{\alpha_N}{\alpha_L}}. \end{cases} \quad (12)$$

As per the association rule in section II-B, the typical user is associated with a single UAV-BS which could be a LoS or a NLoS UAV-BS. The following lemma gives the probabilities that the typical user is either associated with a LoS UAV-BS or a NLoS UAV-BS.

Lemma 2. *The probability that the typical user is associated with a LoS UAV-BS is given by*

$$\begin{aligned} A_L &= 1 - 2\pi\lambda \int_0^\infty z P_N(z) \exp\left(-2\pi\lambda \int_0^{\sqrt{U(z)}} t P_L(t) dt\right) \\ &\quad \times \exp\left(-2\pi\lambda \int_0^z t P_N(t) dt\right) dz, \end{aligned} \quad (13)$$

where $U(z) = \left(\frac{\eta_L}{\eta_N}\right)^{\frac{2}{\alpha_L}} (z^2 + h^2)^{\frac{\alpha_N}{\alpha_L}} - h^2$. The probability that the typical user is associated with a NLoS UAV-BS is $A_N = 1 - A_L$.

Proof. See Appendix B. \square

IV. COVERAGE PROBABILITY

The coverage probability is generally defined as the probability that the SINR is greater than a designated threshold T :

$$P_C = \mathbb{P}(\text{SINR} > T). \quad (14)$$

We begin this section by deriving the Laplace transform of the interference, which is given in Lemma 3.

Lemma 3. *The Laplace transform of the aggregated interference power conditioned on the serving UAV-BS being at a distance r from the typical user is given by*

$$\begin{aligned} \mathcal{L}_I(s|r) = & \exp \left(-2\pi\lambda \int_{v_1(r)}^{\infty} \left[1 - \frac{1}{1 + s\zeta_N(t^2 + h^2)^{\frac{-\alpha_N}{2}}} \right] \right. \\ & \times tP_N(t)dt - 2\pi\lambda \int_{v_2(r)}^{\infty} \left[1 - \left(\frac{m}{m + s\zeta_L(t^2 + h^2)^{\frac{-\alpha_L}{2}}} \right)^m \right] \\ & \left. \times tP_L(t)dt \right), \end{aligned} \quad (15)$$

with

$$\begin{aligned} v_1(r) &= \sqrt{r^2 - h^2}, \quad v_2(r) = \sqrt{d_L^2 - h^2} \quad \text{if } x_o \in \Phi^N \\ v_1(r) &= \sqrt{d_N^2 - h^2}, \quad v_2(r) = \sqrt{r^2 - h^2} \quad \text{if } x_o \in \Phi^L. \end{aligned}$$

Proof. See Appendix C. \square

Now that we have developed expressions for association probabilities and the Laplace transform of the interference, we present the main theorem on the coverage probability.

Theorem 1. *The probability of coverage P_C is given by*

$$P_C = P_{C,L}A_L + P_{C,N}A_N, \quad (16)$$

where $P_{C,L}$ and $P_{C,N}$ are the conditional coverage probabilities given that the typical user is associated with a LoS UAV-BS or a NLoS UAV-BS, respectively, and are given by

$$\begin{aligned} P_{C,L} = & \sum_{k=1}^m \binom{m}{k} (-1)^{k+1} \int_h^{\infty} \exp \left(-k\mu_L\sigma^2 r^{\alpha_L} - 2\pi\lambda \right. \\ & \left. \int_{l(d_N)}^{\infty} \left[1 - \frac{1}{1 + k\mu_L r^{\alpha_L} \zeta_N(t^2 + h^2)^{\frac{-\alpha_N}{2}}} \right] tP_N(t)dt \right. \\ & \left. - 2\pi\lambda \int_{l(r)}^{\infty} \left[1 - \left(\frac{m}{m + k\mu_L r^{\alpha_L} \zeta_L(t^2 + h^2)^{\frac{-\alpha_L}{2}}} \right)^m \right] \right. \\ & \left. tP_L(t)dt \right) f_{R_L}(r)dr, \end{aligned} \quad (17)$$

and

$$\begin{aligned} P_{C,N} = & \int_h^{\infty} \exp \left(-\sigma^2 T \zeta_N^{-1} r^{\alpha_N} - 2\pi\lambda \int_{l(r)}^{\infty} \left[1 - \right. \right. \\ & \left. \left. \frac{1}{1 + T r^{\alpha_N} (t^2 + h^2)^{\frac{-\alpha_N}{2}}} \right] tP_N(t)dt - 2\pi\lambda \int_{l(d_L)}^{\infty} \left[1 - \right. \right. \\ & \left. \left. \left(\frac{m}{m + \eta_N^{-1} \eta_L T r^{\alpha_N} (t^2 + h^2)^{\frac{-\alpha_L}{2}}} \right)^m \right] tP_L(t)dt \right) f_{R_N}(r)dr, \end{aligned} \quad (18)$$

where $\mu_L = \alpha m T \zeta_L^{-1}$, $l(d_N) = \sqrt{d_N^2 - h^2}$, $l(r) = \sqrt{r^2 - h^2}$, and $l(d_L) = \sqrt{d_L^2 - h^2}$.

Proof. See Appendix D. \square

V. AVERAGE ACHIEVABLE RATE

The average achievable rate of the typical user is given by $\tau = \mathbb{E}[\ln(1 + \text{SINR})]$ (nats/Hz), where 1 bit = $\ln(2) = 0.693$ nats [16]. The following theorem presents the main rate theorem.

Theorem 2. *The average downlink rate of a typical user is given by*

$$\tau = \tau_L A_L + \tau_N A_N, \quad (19)$$

where τ_L and τ_N are the average achievable rates given that the typical user is associated with a LoS or a NLoS UAV-BS, respectively, and are given by

$$\begin{aligned} \tau_L = & \sum_{k=1}^m \binom{m}{k} (-1)^{k+1} \int_{r \geq h} \exp(k\rho_L \sigma^2 r^{\alpha_L}) \\ & \int_{y>0} \exp \left(-k\rho_L \sigma^2 r^{\alpha_L} e^y - 2\pi\lambda \int_{l(d_N)}^{\infty} \right. \\ & \left. \left[1 - \frac{1}{1 + k\rho_L r^{\alpha_L} (e^y - 1) \zeta_N(t^2 + h^2)^{\frac{-\alpha_N}{2}}} \right] tP_N(t)dt \right. \\ & \left. - 2\pi\lambda \int_{l(r)}^{\infty} \left[1 - \left(\frac{m}{m + k\alpha m r^{\alpha_L} (e^y - 1) (t^2 + h^2)^{\frac{-\alpha_L}{2}}} \right)^m \right] \right. \\ & \left. tP_L(t)dt \right) f_{R_L}(r)dr, \end{aligned} \quad (20)$$

and

$$\begin{aligned} \tau_N = & \int_{r \geq h} \exp(\sigma^2 \zeta_N^{-1} r^{\alpha_N}) \int_{y>0} \exp \left(-\sigma^2 \zeta_N^{-1} r^{\alpha_N} e^y \right. \\ & \left. - 2\pi\lambda \int_{l(r)}^{\infty} \left[1 - \frac{1}{1 + r^{\alpha_N} (e^y - 1) (t^2 + h^2)^{\frac{-\alpha_N}{2}}} \right] tP_N(t)dt \right. \\ & \left. - 2\pi\lambda \int_{l(d_L)}^{\infty} \left[1 - \left(\frac{m}{m + \zeta_N^{-1} r^{\alpha_N} (e^y - 1) \zeta_L(t^2 + h^2)^{\frac{-\alpha_L}{2}}} \right)^m \right] \right. \\ & \left. tP_L(t)dt \right), \end{aligned} \quad (21)$$

where $\rho_L = \alpha m \zeta_L^{-1}$, $l(d_N) = \sqrt{d_N^2 - h^2}$, $l(r) = \sqrt{r^2 - h^2}$, and $l(d_L) = \sqrt{d_L^2 - h^2}$.

Proof. See Appendix E. \square

VI. NUMERICAL RESULTS

In this section, we provide simulations to evaluate our main analytical results. In particular, we use MATLAB to simulate Theorem 1 and Theorem 2. We consider dense urban area with parameters $a = 12.08$, $b = 0.11$, $\eta_L = 0.69$ and $\eta_N = 0.005$ [6], [14]. We also consider UAV-BSs that transmit their signals at $f_c = 2$ GHz and $P_t = 30$ dBm while the noise power is assumed -174 dBm/Hz. The NLoS and LoS path loss

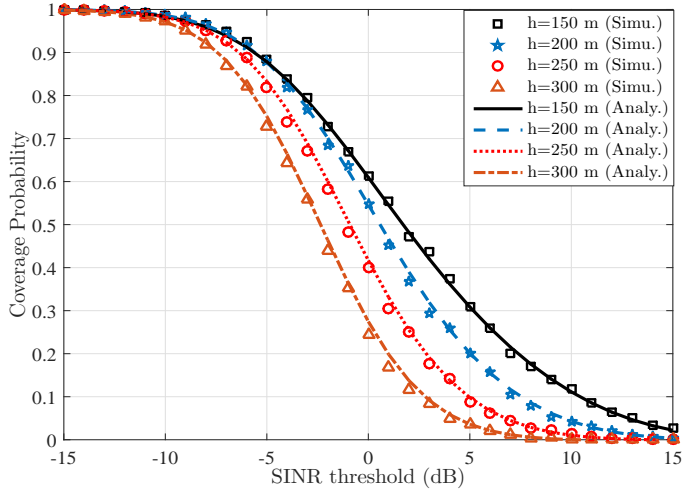


Fig. 2: Coverage probability versus SINR threshold for the typical user for different altitudes.

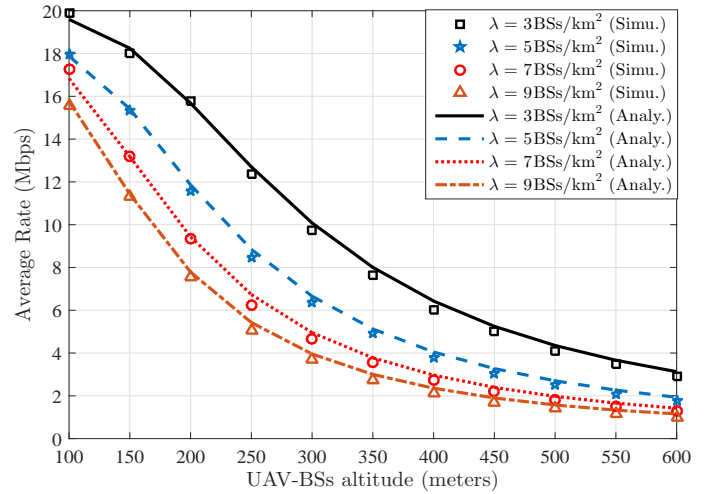


Fig. 3: Average rate versus UAV-BS altitude for the typical user for different UAV-BSs densities (BW=10 MHz).

exponents are $\alpha_N = 3.5$ and $\alpha_L = 2$. The shape parameter of the Nakagami-m fading is $m = 3$ and the system bandwidth is 10 MHz.

The impact of the UAV-BSs altitude on the coverage probability of a typical user is studied in Fig. 2. It can be seen from Fig. 2 that as the UAV-BSs altitude increases, the coverage probability decreases due to the increase in path loss. It can also be observed from Fig. 2 that the analytical results in Theorem 1 match the simulations with negligible errors.

The impact of the UAV-BSs altitude and their densities on the data rate achieved by a typical user are studied in Fig. 3, where we plot the average rate versus UAV-BSs altitude for the UAV-BSs densities $\lambda = 3, 5, 7$ and 9 BSs/km². The results in Fig. 3 show that for a given density, the average achievable rate degrades as the UAV-BSs altitude increases due to the increase in the path loss. Furthermore, for a given UAV-BS altitude, the average achievable rate decreases as the UAV-BSs density increases. This is because the interfering UAV-BSs become closer to the typical user as the density increases which degrades the SINR at the typical user.

VII. CONCLUSION

In this paper, we proposed a stochastic geometry framework to analyze coverage and rate in a network of UAV-BSs deployed at a particular height. The framework accommodates both LoS and NLoS transmissions, and considers Rayleigh fading and Nakagami-m fading for NLoS and LoS links, respectively. We derived analytical expressions for the conditional Laplace transform of the interference power, the association probabilities, and the distribution of the distances between the typical user and the closest NLoS and LoS UAV-BSs. Approximate expressions for the coverage probability and average achievable rate were also derived. Interestingly, we showed that these approximations match the simulations with negligible errors.

APPENDIX A PROOF OF LEMMA 1

Given that R_N is a random variable, the corresponding horizontal Euclidean distance, denoted by Z_N , is also a random variable given by $Z_N = \sqrt{R_N^2 - h^2}$. The cumulative distribution function (CDF) of R_N is given by

$$F_{R_N}(r) = 1 - \mathbb{P}(R_N > r) = 1 - \mathbb{P}\left(Z_N > \sqrt{r^2 - h^2}\right) \\ \stackrel{(a)}{=} 1 - \exp\left(-2\pi\lambda \int_0^{\sqrt{r^2 - h^2}} z P_N(z) dz\right), \quad (22)$$

where (a) follows from the null probability of the PPP [16]. Finally, $f_{R_N}(r) = \frac{d}{dr} F_{R_N}(r)$ which completes the proof of $f_{R_N}(r)$. By following the same steps as for $f_{R_N}(r)$, we can complete the proof of $f_{R_L}(r)$.

APPENDIX B PROOF OF LEMMA 2

Since the UAV-BS that provides the strongest average SINR also provides the strongest average received power [17], the probability that the typical user is associated with a LoS UAV-BS is then given by

$$A_L = \mathbb{P}(\zeta_L R_L^{-\alpha_L} > \zeta_N R_N^{-\alpha_N}) \\ \stackrel{(a)}{=} \mathbb{P}\left(Z_L^2 < \left(\frac{\eta_L}{\eta_N}\right)^{\frac{2}{\alpha_L}} (Z_N^2 + h^2)^{\frac{\alpha_N}{\alpha_L}} - h^2\right) \\ \stackrel{(b)}{=} \int_0^\infty (1 - \mathbb{P}(Z_L^2 > U(z))) f_{Z_N}(z) dz \\ \stackrel{(c)}{=} 1 - \int_0^\infty \mathbb{P}(Z_L > \sqrt{U(z)}) f_{Z_N}(z) dz \\ \stackrel{(d)}{=} 1 - \int_0^\infty \exp\left(-2\pi\lambda \int_0^{\sqrt{U(z)}} t P_L(t) dt\right) f_{Z_N}(z) dz, \quad (23)$$

where (a) is due to $R_L = \sqrt{Z_L^2 + h^2}$ and $R_N = \sqrt{Z_N^2 + h^2}$, (b) follows from conditioning on $Z_N = z$, and $U(z) = \left(\frac{\eta_L}{\eta_N}\right)^{\frac{2}{\alpha_L}} (z^2 + h^2)^{\frac{\alpha_N}{\alpha_L}} - h^2$, (c) follows from the fact that Z_N is a positive random variable, and (d) follows from the null probability of the PPP. Finally, by substituting (8) into (d), we complete the proof.

APPENDIX C PROOF OF LEMMA 3

The Laplace transform $\mathcal{L}_I(s)$ can be written as follows:

$$\begin{aligned} \mathcal{L}_I(s) &= \mathbb{E}_I[\exp(-sI)] \\ &\stackrel{(a)}{=} \mathbb{E}_{\phi^N} \left[\prod_{x_i \in \phi^N \setminus x_o} \mathbb{E}_H \exp\left(-s\zeta_N H_{x_i} D_{N,x_i}^{-\alpha_N}\right) \right] \\ &\quad \times \mathbb{E}_{\phi^L} \left[\prod_{x_i \in \phi^L \setminus x_o} \mathbb{E}_G \exp\left(-s\zeta_L G_{x_i} D_{L,x_i}^{-\alpha_L}\right) \right] \\ &= \mathbb{E}_{\phi^N} \left[\prod_{x_i \in \phi^N \setminus x_o} \frac{1}{1 + s\zeta_N D_{N,x_i}^{-\alpha_N}} \right] \\ &\quad \times \mathbb{E}_{\phi^L} \left[\prod_{x_i \in \phi^L \setminus x_o} \left(\frac{m}{m + s\zeta_L D_{L,x_i}^{-\alpha_L}} \right)^m \right], \quad (24) \end{aligned}$$

where (a) follows from (4), the i.i.d distribution and the independence of the spatial point process and small scale fading.

Now given that the typical user is associated with a NLoS UAV-BS (i.e., $x_o \in \Phi^N$) located at a distance $R_N = r$, and from Remark (1) and the probability generating functional (PGFL) of the PPP, we obtain the final result in (15) for the case $x_o \in \Phi^N$. Similarly, the conditional Laplace transform of the aggregated interference power when the typical user is associated with a LoS UAV-BS can be obtained from remark (2) and the PGFL of the PPP.

APPENDIX D PROOF OF THEOREM 1

Given that the typical user is associated with a LoS UAV-BS, the conditional coverage probability $P_{C,L}$ is given by

$$\begin{aligned} P_{C,L} &= \mathbb{P}\left(\frac{\zeta_L G_{x_o} R_L^{-\alpha_L}}{\sigma^2 + I} > T\right) \\ &\stackrel{(a)}{=} \int_h^\infty \mathbb{P}(G_{x_o} > T\zeta_L^{-1} r^{\alpha_L} (\sigma^2 + I)) f_{R_L}(r) dr \\ &\stackrel{(b)}{=} 1 - \int_h^\infty \mathbb{E}_I[F_G(T\zeta_L^{-1} r^{\alpha_L} (\sigma^2 + I))] f_{R_L}(r) dr \\ &\stackrel{(c)}{=} 1 - \int_h^\infty \mathbb{E}_I\left[\frac{\Gamma_l(m, mT\zeta_L^{-1} r^{\alpha_L} (\sigma^2 + I))}{\Gamma(m)}\right] f_{R_L}(r) dr, \quad (25) \end{aligned}$$

where (a) follows from conditioning on the serving LoS UAV-BS being at a distance $R_L = r$ from the typical user, (b) follows from the definition $F_G(g) = \mathbb{P}(G \leq g)$ and taking the conditional expectation with respect to interference, and (c) follows from the definition of the CDF of Gamma distribution $F_G(g) = \frac{\Gamma_l(m, mg)}{\Gamma(m)}$ where $\Gamma_l(m, mg) = \int_0^{mg} t^{m-1} e^{-t} dt$ is the lower incomplete gamma function.

The evaluation of the CDF of Gamma distribution requires evaluating higher order derivatives of the Laplace transform. The larger the shape parameter m is, the higher the evaluation complexity is. Therefore, in the following, we provide an approximate evaluation of the coverage probability. In particular, we use a tight bound for the CDF of the Gamma distribution rather than using the exact evaluation. The CDF of Gamma distribution can be bounded as [18]

$$(1 - e^{-\beta mg})^m < \frac{\Gamma_l(m, mg)}{\Gamma(m)} < (1 - e^{-\alpha mg})^m, \quad (26)$$

where $m \neq 1$, and

$$\beta = \begin{cases} 1, & \text{if } m > 1 \\ (m!)^{\frac{-1}{m}}, & \text{if } m < 1 \end{cases} \quad \alpha = \begin{cases} (m!)^{\frac{1}{m}}, & \text{if } m > 1 \\ 1, & \text{if } m < 1. \end{cases} \quad (27)$$

It has been shown in [19] that the upper bound in (26) provides a good approximation to the CDF of Gamma distribution. Therefore, we use the tighter upper bound. The conditional coverage probability can then be written as

$$\begin{aligned} P_{C,L} &\approx 1 - \int_h^\infty \mathbb{E}_I[(1 - \exp(-\mu_L r^{\alpha_L} (\sigma^2 + I)))^m] \\ &\quad \times f_{R_L}(r) dr \\ &\stackrel{(a)}{=} \int_h^\infty \mathbb{E}_I\left[\sum_{k=1}^m \binom{m}{k} (-1)^{k+1} \exp(-k\mu_L r^{\alpha_L} (\sigma^2 + I))\right] \\ &\quad \times f_{R_L}(r) dr \\ &\stackrel{(b)}{=} \int_h^\infty \sum_{k=1}^m \binom{m}{k} (-1)^{k+1} \exp(-k\mu_L \sigma^2 r^{\alpha_L}) \\ &\quad \times \mathbb{E}_I[\exp(-k\mu_L r^{\alpha_L} I)] f_{R_L}(r) dr \\ &= \sum_{k=1}^m \binom{m}{k} (-1)^{k+1} \int_h^\infty \exp(-k\mu_L \sigma^2 r^{\alpha_L}) \\ &\quad \times \mathcal{L}_I(k\mu_L r^{\alpha_L}) f_{R_L}(r) dr, \quad (28) \end{aligned}$$

where $\mu_L = \alpha m T \zeta_L^{-1}$, (a) follows from the binomial theorem and the assumption that m is an integer, and (b) results from the linearity of the expectation. Finally, $\mathcal{L}_I(k\mu_L \sigma^2 r^{\alpha_L})$ is obtained from (15) where $v_1(r) = \sqrt{d_N^2 - h^2}$ and $v_2(r) = \sqrt{r^2 - h^2}$ which completes the proof of (17). Similarly, $P_{C,N}$ can be derived by following the same approach as that of $P_{C,L}$ and by setting $m = 1$. Therefore, we omit the detailed proof of (18).

APPENDIX E PROOF OF THEOREM 2

The average achievable rate is given by

$$\begin{aligned} \tau &= \mathbb{E}[\ln(1 + \text{SINR})] \stackrel{(a)}{=} \int_{y>0} \mathbb{P}(\ln(1 + \text{SINR}) > y) dy \\ &\stackrel{(b)}{=} \int_{y>0} \mathbb{P}(\ln(1 + \text{SINR}) > y | x_o \in \Phi^L) dy A_L + \\ &\quad \int_{y>0} \mathbb{P}(\ln(1 + \text{SINR}) > y | x_o \in \Phi^N) dy A_N \\ &= \tau_L A_L + \tau_N A_N, \quad (29) \end{aligned}$$

where (a) follows from the fact that for a positive random variable X , we have $\mathbb{E}[X] = \int_{y>0} \mathbb{P}(X > y) dy$ [16], and

(b) follows from the law of total probability and linearity of integrals. Now, given that the typical user is associated with a LoS UAV-BS, the conditional average rate is given by

$$\begin{aligned}
\tau_L &\stackrel{(a)}{=} \int_{y>0} \mathbb{P} \left(\ln \left(1 + \frac{\zeta_L G_{x_o} R_L^{-\alpha_L}}{\sigma^2 + I} \right) > y \right) dy \\
&\stackrel{(b)}{=} \int_{y>0} \int_{r \geq h} \mathbb{E}_I \left[\mathbb{P} \left(G_{x_o} > \zeta_L^{-1} r^{\alpha_L} (e^y - 1) (\sigma^2 + I) \right) \right] \\
&\quad \times f_{R_L}(r) dr dy \\
&\stackrel{(c)}{=} \int_{y>0} \int_{r \geq h} \mathbb{E}_I \left[1 - (1 - \exp(-\rho_L r^{\alpha_L} (e^y - 1) (\sigma^2 + I)))^m \right] \\
&\quad \times f_{R_L}(r) dr dy \\
&\stackrel{(d)}{=} \int_{y>0} \int_{r \geq h} \mathbb{E}_I \left[\sum_{k=1}^m \binom{m}{k} (-1)^{k+1} \right. \\
&\quad \left. \exp(-k \rho_L r^{\alpha_L} (e^y - 1) (\sigma^2 + I)) \right] f_{R_L}(r) dr dy \\
&\stackrel{(e)}{=} \sum_{k=1}^m \binom{m}{k} (-1)^{k+1} \int_{y>0} \int_{r \geq h} \exp(-k \rho_L \sigma^2 r^{\alpha_L} (e^y - 1)) \\
&\quad \mathbb{E}_I [\exp(-k \rho_L r^{\alpha_L} (e^y - 1) I)] f_{R_L}(r) dr dy \\
&\stackrel{(f)}{=} \sum_{k=1}^m \binom{m}{k} (-1)^{k+1} \int_{r \geq h} \exp(k \rho_L \sigma^2 r^{\alpha_L}) \\
&\quad \times \int_{y>0} \exp(-k \rho_L \sigma^2 r^{\alpha_L} e^y) \mathcal{L}_I(k \rho_L r^{\alpha_L} (e^y - 1)) dy f_{R_L}(r) dr,
\end{aligned}$$

where $\rho_L = \alpha m \zeta_L^{-1}$, (a) follows from (3), (b) follows from conditioning on $R_L = r$ and taking the conditional expectation with respect to interference, (c) is from the upper bound of Gamma distribution given in (26), (d) results from the binomial theorem and the assumption that m is an integer, (e) follows from the linearity of integrals and expectation, and the last step results from swapping the integration orders. Finally, plugging (15) into (f) when $s = k \rho_L r^{\alpha_L} (e^y - 1)$ completes the proof of (20). The average achievable rate given that the typical user is associated with a NLoS UAV-BS (τ_N) can be derived by following the same approach as that of τ_L and by setting $m = 1$. Therefore, we omit the detailed proof of (21).

REFERENCES

- [1] X. Cao, P. Yang, M. Alzenad, X. Xi, D. Wu, and H. Yanikomeroglu, "Airborne communication networks: A survey," *IEEE J. Select. Areas Commun.*, vol. PP, no. 99, pp. 1–1, 2018, DOI:10.1109/JSAC.2018.2864423.
- [2] I. Bor-Yaliniz, A. El-Keyi, and H. Yanikomeroglu, "Spatial configuration of agile wireless networks with drone-BSs and user-in-the-loop," to appear in *IEEE Trans. Wireless Commun.*, vol. PP, no. 99, pp. 1–1.
- [3] M. Alzenad, M. Z. Shakir, H. Yanikomeroglu, and M.-S. Alouini, "FSO-based vertical backhaul/fronthaul framework for 5G+ wireless networks," *IEEE Commun. Mag.*, vol. 56, no. 1, pp. 218–224, 2018.
- [4] Y. Zeng, R. Zhang, and T. J. Lim, "Wireless communications with unmanned aerial vehicles: Opportunities and challenges," *IEEE Commun. Mag.*, vol. 54, no. 5, pp. 36–42, May 2016.
- [5] I. Bor-Yaliniz and H. Yanikomeroglu, "The new frontier in RAN heterogeneity: Multi-tier drone-cells," *IEEE Commun. Mag.*, vol. 54, no. 11, pp. 48–55, Nov. 2016.
- [6] M. Alzenad, A. El-Keyi, F. Lagum, and H. Yanikomeroglu, "3D placement of an unmanned aerial vehicle base station (UAV-BS) for energy-efficient maximal coverage," *IEEE Wireless Commun. Lett.*, vol. 6, no. 4, pp. 434–437, Aug. 2017.

- [7] M. Alzenad, A. El-Keyi, and H. Yanikomeroglu, "3D placement of an unmanned aerial vehicle base station for maximum coverage of users with different QoS requirements," *IEEE Wireless Commun. Lett.*, vol. 7, no. 1, pp. 38–41, Feb. 2018.
- [8] E. Kalantari, M. Z. Shakir, H. Yanikomeroglu, and A. Yongacoglu, "Backhaul-aware robust 3D drone placement in 5G+ wireless networks," in *Proc. IEEE Int. Conf. Commun. Workshop (ICCW)*, Paris, France, May 2017.
- [9] M. Mozaffari, W. Saad, M. Bennis, and M. Debbah, "Efficient deployment of multiple unmanned aerial vehicles for optimal wireless coverage," *IEEE Commun. Lett.*, vol. 20, no. 8, pp. 1647–1650, Aug. 2016.
- [10] B. Galkin, J. Kibilda, and L. A. DaSilva, "Coverage analysis for low-altitude UAV networks in urban environments," in *Proc. IEEE Glob. Commun. Conf. (Globecom)*, Singapore, Dec. 2017.
- [11] V. V. Chetlur and H. S. Dhillon, "Downlink coverage analysis for a finite 3-D wireless network of unmanned aerial vehicles," *IEEE Trans. Commun.*, vol. 65, no. 10, pp. 4543–4558, Oct. 2017.
- [12] C. Zhang and W. Zhang, "Spectrum sharing for drone networks," *IEEE J. Select. Areas Commun.*, vol. 35, no. 1, pp. 136–144, Jan. 2017.
- [13] X. Zhou, J. Guo, S. Durrani, and H. Yanikomeroglu, "Uplink coverage performance of an underlay drone cell for temporary events," in *Proc. IEEE Int. Conf. Commun. (ICC)*, Kansas City, USA, May 2018.
- [14] A. Al-Hourani, S. Kandeepan, and S. Lardner, "Optimal LAP altitude for maximum coverage," *IEEE Wireless Commun. Lett.*, vol. 3, no. 6, pp. 569–572, Dec. 2014.
- [15] D. Wackerly, W. Mendenhall, and R. Scheaffer, *Mathematical Statistics with Applications*, 2007.
- [16] J. G. Andrews, F. Baccelli, and R. K. Ganti, "A tractable approach to coverage and rate in cellular networks," *IEEE Trans. Commun.*, vol. 59, no. 11, pp. 3122–3134, Nov. 2011.
- [17] B. Yang, G. Mao, M. Ding, X. Ge, and X. Tao, "Dense small cell networks: From noise-limited to dense interference-limited," *IEEE Trans. Veh. Technol.*, vol. 67, no. 5, pp. 4262–4277, May 2018.
- [18] H. Alzer, "On some inequalities for the incomplete Gamma function," *Math. Comput.*, vol. 66, no. 218, pp. 771–778, 1997.
- [19] T. Bai and R. W. Heath, "Coverage and rate analysis for millimeter-wave cellular networks," *IEEE Trans. Wireless Commun.*, vol. 14, no. 2, pp. 1100–1114, Feb. 2015.